Online Robust Fatigue Tracking Algorithms for Wearable sEMG Systems in Noisy Environments

Mert Ergeneci, Kaan Gokcesu, Erhan Ertan, Hakan Gokcesu, Panagiotis Kosmas

***Abstract*—Muscle fatigue can be tracked through surface electromyography technology (sEMG). There are several approaches in literature for detecting muscular exhaustion. Since the muscle fatigue can be straightforwardly tracked by the spectral shift of the EMG signal, the most widely used techniques generally include the frequency domain approaches, i.e., spectral methods. However, these techniques have certain limitations and may provide poor performance, especially under low SNR scenarios where the additive white Gaussian noise (AWGN) power is high. This shortcoming is most apparent in the two most popular techniques for tracking muscular fatigue: mean frequency tracking and median frequency tracking. In both mean and median frequency techniques to track the spectral shift, a certain increase in the AWGN power can give deceiving results since it can disrupt the noise-free mean and median frequency. To this end, we propose novel algorithms to track the spectral shift. These methods are very robust against noise environments and they are negligibly affected by the high noise or AWGN power. Through several experiments, we validated our algorithms and illustrated better performance against the conventional methods. Moreover, in the experiments, we increased AWGN power up to 60 dB gradually, and observed a maximum of 6 Hz and 2 Hz of overall change in our proposed methods, while other methods showed frequency change between 30 Hz and 90 Hz.**

I. Introduction

Muscle fatigue is the inability of the muscle to generate the desired contraction and force, as a result of repetitive and power-exhaustive tasks [1], [2]. The detection and tracking of muscle fatigue has gained significant attention in the sports science and rehabilitation applications. It can be used in various scenarios, including but not limited to the prevention of muscle injury, over-training and re-injury during rehabilitation; the analysis of muscle strength and endurance development; and the monitoring of the gradual athlete performance [3]–[11].

Surface electromyography (sEMG), which is an electrodiagnostic, non-invasive medical technology used in evaluating and recording the electrical activity produced by skeletal muscles [12]. sEMG has been proven to be a substantial technology to track the muscular fatigue since it can monitor the muscle activation potentials. The effects of muscle fatigue on the muscle activation potentials are significant, hence, the sEMG signal is a paramount tool in the analysis of the muscle fatigue.

There are several methods to track the muscle fatigue that make use of the sEMG technology. These methods are generally divided into two main categories: frequency-domain approaches and time-domain approaches. However, because of the spectral shift encountered under muscular fatigue, the frequency-domain (spectral) approaches has been widely popular.

The power spectral density (PSD) of the sEMG signal (which is the distribution of the power of the sEMG signal across different frequency components) has a certain nonrandom waveform behavior. The PSD of the sEMG signal is dominant in the frequency band of 30-150 Hz. After approximately 200 Hz, the spectral power of the sEMG signal diminishes and only the power of the AWGN remains. When the muscles start to get exhausted, the lactate and other ions such as H^+, Ca^{+2}, Na^+, and P^{-3} start to accumulate, which lessens the conductivity in the motor units of the muscle [13]–[15]. Thus, the total number of impulses passing through the motor units of the muscle during a specific time interval decreases. Therefore, when the muscle is fatigued, the dominant part of the PSD tends to shift to the lower frequency components.

In particular, methods such as mean frequency and median frequency analysis of the PSD of the sEMG signal has gained wide popularity since they can straightforwardly track the shift in the spectra that is caused by the fatigue. These methods are the most prominent of the frequency-based techniques of the state of the art [16]–[21]. However, the results of such metrics can be greatly affected by the AWGN power. Hence, muscle fatigue tracking with such methods can give misleading results, especially when the AWGN power is very high or is prone to change [22], [23]. In this paper, we detail this problem that is encountered by not just the mean and median frequency but most of the EMG-based fatigue tracking metrics.

To this end, in order to overcome this obstacle, we propose two new approaches, which are the discrete derivative analysis (DDA), and the cumulative sigmoid analysis (CSA). These methods can accurately calculate the shift in the PSD of the sEMG signal in a very robust manner, regardless of the amount or change in the AWGN power.

The remainder of the paper is organized as follows. In Section II, we give the necessary preliminaries. In Section III, we detail the spectral shift analysis methods in literature by focusing on the mean and median frequency tracking. In Section IV, we explain in detail our novel algorithms that can track the shift in the spectra in a robust manner. Next, in Section V, the experiments of the proposed methods are

M. Ergeneci and E. Ertan is with Neurocess R&D Labs, Shenzhen, Guangdong, China, (e-mail: ergenecimert@gmail.com, erhertan@gmail.com).

K. Gokcesu is with the Department of Electrical Engineering and Computer Science, Cambridge, MA 02139, USA, (e-mail:gokcesu@mit.edu).

H. Gokcesu is with the Department of Electrical and Electronics Engineering, 06800, Bilkent, Ankara, Turkey, (e-mail:hgokcesu@ee.bilkent.edu.tr).

P. Kosmas is with the School of Natural and Mathematical Sciences, King's College London, London WC2R 2LS, U.K. (e-mail: panagiotis.kosmas@kcl.ac.uk).

demonstrated, where we first validate our metrics' ability to model the muscular fatigue and then show that our algorithms are much more robust against the noise power in the environment in comparison to the conventional techniques. Finally, some concluding remarks are given in Section VI.

II. Preliminaries

In this section, we first provide some necessary preliminaries for the problem that we are dealing with, which is the tracking of the muscular fatigue through sEMG signal analysis. First of all, we formally define what constitutes an sEMG signal and provide its mathematical model in the subsequent subsection.

A. sEMG Signal Model

An sEMG signal can be mathematically modeled as the following:

$$y[n] = x[n] + v[n], \tag{1}$$

where $y[n]$ is the observed sEMG output, $x[n]$ is the muscle activation potential and $v[n]$ is the AWGN noise.

Generally, in the most prominent sEMG applications, the frames of the sEMG data are processed. Since in real-time systems, the processing of the whole stream is infeasible and a single measurement (sample-by-sample) carries very little information, the applications generally use a sliding window [23]–[29].

To this end, let N be the frame length and L be the overlap length (the two adjacent frames have in common a total of L samples). We define the column vector $\boldsymbol{y}_t$ as the frame at time t which is

$$\boldsymbol{y}_t = \left[y[m+1], y[m+2], \ldots, y[m+N]\right]^T, \tag{2}$$

where $m = (t-1)(N-L)$. The column vectors $\boldsymbol{x}_t, \boldsymbol{v}_t$ are similarly defined as the frames at time t of the clean EMG signal and AWGN noise respectively. We also define the half length Discrete Fourier Transforms (DFT) of these column vectors as $\boldsymbol{Y}_t, \boldsymbol{X}_t, \boldsymbol{V}_t$ respectively. Hence,

$$\boldsymbol{y}_t = \boldsymbol{x}_t + \boldsymbol{v}_t, \tag{3}$$

$$\boldsymbol{Y}_t = \boldsymbol{X}_t + \boldsymbol{V}_t. \tag{4}$$

Note that if there is no contraction at time t, then the observation frame is simply given by $\boldsymbol{Y}_t = \boldsymbol{V}_t$. Therefore, we can write the model in a more concise form as

$$\boldsymbol{y}_t = \alpha_t \boldsymbol{s}_t + \boldsymbol{v}_t, \tag{5}$$

$$\boldsymbol{Y}_t = \alpha_t \boldsymbol{S}_t + \boldsymbol{V}_t, \tag{6}$$

where $\boldsymbol{S}_t$ is the muscle contraction signal, $\boldsymbol{X}_t = \alpha_t \boldsymbol{S}_t$ and α_t is 1 if there is a contraction and 0 otherwise. We point out that the detection of the contractions are very important for reliable analysis of the sEMG signal since only from the frames where $\alpha_t = 1$, we can infer something about the muscle activation potentials (i.e., $\boldsymbol{S}_t$) from the observed signal $\boldsymbol{Y}_t$. Hence, in the next subsection, we provide an algorithm whose sole purpose is the detection of these contraction frames.

B. Contraction Detection

As can be seen, the muscle contraction signal $\boldsymbol{s}_t$ is present inside $\boldsymbol{y}_t$ only when there is a contraction, i.e., $\alpha_t = 1$. Therefore, we need to first detect the contractions to track the muscular fatigue. This is actually true for all the fatigue tracking methods since when there are no contractions, the observed signal is simply AWGN and provides no value to us. If included in the analysis, the metrics extracted from the noise frames can actually degrade the performance of the algorithms.

To detect the contraction frames, we use a modified version of the contraction detection algorithm in [29], where we use the power p_t of the incoming observation frame $\boldsymbol{y}_t$, which is

$$p_t = \boldsymbol{y}_t^T \boldsymbol{y}_t. \tag{7}$$

We train a threshold value τ_t, which we use to compare against the power p_t of the t^{th} observation frame. If the power p_t is greater than the threshold τ_t, we detect a contraction (i.e., $\alpha_t = 1$) and label the frame as noise (i.e., $\alpha_t = 0$) otherwise, i.e.,

$$\alpha_t = \begin{cases} 1, & p_t > \tau_t \text{ (active)} \\ 0, & p_t \leq \tau_t \text{ (inactive)} \end{cases}. \tag{8}$$

We update the threshold by taking the cumulative geometric mean of the power of incoming frames p_t. Hence, it is sequentially calculated as

$$\tau_{t+1} = \exp\left(\log(\tau_t) - (\log(\tau_t) - \log(p_t))/t\right) \tag{9}$$

Similarly, other metrics can also be used instead of the power of the incoming frames. The approach in [29] can be modified in a variety of ways. As an example, instead of the cumulative geometric mean, cumulative arithmetic mean can also be used. However, note that, if there are a lot of active frames in the measured EMG data, this mean can be undesirably high, which may cause the algorithm to misclassify contraction frames as noise since some contractions may have lower frame energies. Therefore, we need a substantially lower threshold level. Since the noise frame energies are generally similar and comparably lower to the active frames, we need a threshold value nearer to the minimum received frame energy. That is the reason we use geometric mean.

After correctly detecting the contraction frames, we can process them in order to track the muscular fatigue. With the contraction frames at hand, we need some way of quantifying the fatigue level in the muscle. In the next subsection, we explain the necessary qualities of a fatigue tracking metric.

C. Fatigue Metric

The muscle contraction signal $\boldsymbol{s}_t$ has a direct relationship to the current muscular fatigue f_t, such that the muscular fatigue f_t is a function of the muscle contraction signal $\boldsymbol{s}_t$. Our main goal is to produce an estimate $\hat{f}_t$ from the noisy signal $\boldsymbol{y}_t$.

We first note that the definition of fatigue is actually very vague and arbitrary. Generally, there is no universally agreed on metric for muscular fatigue. Nonetheless, since the thing of interest is mainly the change in the fatigue, a consistent metric is sufficient for fatigue tracking purposes as long as the change in its value corresponds to a similar behavior.

For this purpose, let $F(\cdot)$ be some metric that we believe satisfactorily models the muscular fatigue, i.e., let

$$f_t = F(\boldsymbol{s}_t), \tag{10}$$

$$\hat{f}_t = F(\boldsymbol{y}_t). \tag{11}$$

Since we are mainly interested in the spectral analysis methods, we have

$$f_t = F(\boldsymbol{S}_t), \tag{12}$$

$$\hat{f}_t = F(\boldsymbol{Y}_t). \tag{13}$$

As we can see from the equations there are two important considerations that needs to be made. Obviously, the first is that $f_t = F(\boldsymbol{S}_t)$ can closely model the muscular fatigue as we believe at least in the behavioral sense. Secondly, the estimate $\hat{f}_t$ is as close to the f_t as possible. We deal with the first consideration in the first part of the experiments where we compare the waveforms against the well established conventional fatigue tracking algorithms. We deal with the second consideration in the second part of the experiments, where we will show that our algorithms are much more robust against the noise $\boldsymbol{v}_t$. In the next section, we first detail the most popular conventional methods in the literature.

III. Conventional Techniques: Tracking the Central Tendency of the Spectra

In this section, we explain the conventional methods to track the shift in the spectral behavior of the acquired contraction frames. The change in the spectral behavior gives us the change in the localized fatigue level. In Section IV, we propose two methods related to tracking the shift of the spectrum and compare them with four state of the art metrics in the experiments, which we detail here. These methods are the mean frequency, the median frequency, the band-limited mean frequency and the band-limited median frequency. Thus, in the following subsections we will explain in detail the mean and median frequency and how they are affected by the AWGN noise power. For the purposes of the succeeding sections, let $\boldsymbol{y}_t$ be the received t^{th} frame, which contains contraction, i.e., $\alpha_t = 1$. Let $\boldsymbol{Y}_t$ be the Discrete Time Fourier Transform (DFT) of $\boldsymbol{y}_t$. Then the PSD of $\boldsymbol{y}_t$ (i.e., $\boldsymbol{P}_t$) is calculated as the square of the magnitude of $\boldsymbol{Y}_t$ of each frequency bin normalized to a probability simplex, i.e.,

$$\boldsymbol{P}_t[k] = \frac{\|\boldsymbol{Y}_t[k]\|^2}{\sum_{k=0}^{K} \|\boldsymbol{Y}_t[k]\|^2}, \tag{14}$$

where K is the frequency bin corresponding to half the sampling rate, i.e., the Nyquist frequency, and the summation of $\boldsymbol{P}_t$ gives 1.

A. Mean Frequency

The mean frequency, i.e., MN_t, of the t^{th} frame is calculated as the sum of the PSD values multiplied by their frequency content. Hence, MN_t is calculated as follows

$$MN_t = \sum_{k=0}^{K} k\boldsymbol{P}_t[k], \tag{15}$$

which gives the average of the random variable whose probability mass function corresponds to the PSD, $\boldsymbol{P}_t$, of $\boldsymbol{Y}_t$.

1) Effect of the AWGN Power: Let p_s be the power of the sEMG signal and p_v be the power of the AWGN noise. Since AWGN noise is distributed among the frequency components equally in expectation, the mean frequency of the noise power will be given by $K/2$. Hence, the estimate of the mean frequency is given by

$$\widehat{MN}_t = \frac{p_s}{p_s + p_v} MN_t + \frac{p_v}{p_s + p_v} \frac{K}{2}, \tag{16}$$

$$= MN_t + \frac{p_v}{p_s + p_v} \left(K/2 - MN_t\right). \tag{17}$$

Thus, the deviation from the true mean frequency will be

$$\left\| \widehat{MN}_t - MN_t \right\| = \frac{p_v}{p_s + p_v} \left\| K/2 - MN_t \right\|. \tag{18}$$

Hence, in high SNR, i.e., $p_v << p_s$, this is not an issue since $\frac{p_v}{p_s+p_v} \to 0$. However, in low SNR scenarios, i.e., $p_v >> p_s$, the deviation can be substantial since $\frac{p_v}{p_s+p_v} \to 1$.

B. Band-limited Mean Frequency

The band-limited mean frequency, i.e., BMN_t, of the t^{th} frame is calculated as the sum of the PSD values of the frequency components in the passband multiplied by their frequency content. Hence, BMN_t is calculated as follows

$$BMN_t = \frac{\sum_{k=k_1}^{k_2} k\boldsymbol{P}_t[k]}{\sum_{k=k_1}^{k_2} \boldsymbol{P}_t[k]}, \tag{19}$$

where k_1 and k_2 are the limits of the passband. Hence, BMN_t gives the average of the random variable whose probability mass function (PMF) corresponds to the normalized version of the PSD between the frequency bins k_1 to k_2.

1) Effect of the AWGN Power: The effect is similar to the case in Section III-A.

C. Median Frequency (MDF)

In order to estimate the median frequency of the t^{th} window, MD_t, we calculate the cumulative sum $\boldsymbol{C}_t$ of $\boldsymbol{P}_t$ as

$$\boldsymbol{C}_t[k] = \sum_{k'=0}^{k} \boldsymbol{P}_t[k'], \tag{20}$$

for $k \in \{0, 1, 2, \ldots, K\}$. Let k^* be the index of the first component in $\boldsymbol{C}_t$ that is greater than 0.5, i.e.,

$$\boldsymbol{C}_t[k^*] > \frac{1}{2}, \tag{21}$$

$$\boldsymbol{C}_t[k^* - 1] \leq \frac{1}{2}. \tag{22}$$

Then, MD_t is given by

$$MD_t = k^* - 1 + \frac{0.5 - \boldsymbol{C}_t[k^* - 1]}{\boldsymbol{C}_t[k^*] - \boldsymbol{C}_t[k^* - 1]}, \tag{23}$$

$$= k^* - \frac{\boldsymbol{C}_t[k^*] - 0.5}{\boldsymbol{C}_t[k^*] - \boldsymbol{C}_t[k^* - 1]} \tag{24}$$

1) Effect of the AWGN Power: Let again p_s be the power of the sEMG signal and p_v be the power of the AWGN noise. In high SNR cases, i.e., $p_v << p_s$, and $\frac{p_v}{p_s+p_v} \to 0$, the median frequency will be biased towards the median frequency of AWGN albeit slightly. Hence, it will not be an issue. However, in low SNR scenarios, i.e., $p_v >> p_s$, and $\frac{p_v}{p_s+p_v} \to 1$, the median frequency will be substantially tilted towards the median frequency of AWGN, which is $(K-1)/2$.

D. Band-limited Median Frequency (MDF)

Let again k_1 and k_2 be the limits of the passband. In order to estimate the band-limited median frequency of the t^{th} window, denoted BMD_t, the band-limited cumulative sum $\boldsymbol{BC}_t$ of the $\boldsymbol{P}_t$ is taken such that

$$\boldsymbol{BC}_t[k] = \frac{\sum_{k'=k_1}^{k} \boldsymbol{P}_t[k']}{\sum_{k'=k_1}^{k_2} \boldsymbol{P}_t[k']}, \tag{25}$$

for $k \in \{k_1, \ldots, k_2\}$. Let again k^* be the index of the first component in $\boldsymbol{BC}_t$ that is greater than 0.5. Then, BMD_t is

$$BMD_t = k^* - \frac{\boldsymbol{BC}_t[k^*] - 0.5}{\boldsymbol{BC}_t[k^*] - \boldsymbol{BC}_t[k^*-1]} \tag{26}$$

1) Effect of the AWGN Power: The effect is similar to the case in Section III-C.

IV. Robust Methods: Tracking the Stopband of the Spectra

In this section, we explain our algorithms and the metrics that we propose to track the muscular fatigue using the sEMG data. We propose two algorithms, which are the Discrete Derivative Analysis (DDA) and Cumulative Sigmoid Analysis (CSA). We first explain in detail the DDA approach.

A. Discrete Derivative Analysis

In this method, we track the frequency index, where the dominance of the PSD of the sEMG signal is finished. By this way, the spectrum shift during muscular fatigue becomes traceable no matter how much AWGN is present.

The expected PSD is given by the summation of the power spectra of the muscle signal and the power spectra of the AWGN noise. The AWGN noise is constant throughout the spectra. When the discrete derivative is taken, the parts of the spectra where the signal power is negligible will converge to zero. Since the discrete derivative simulates the derivative of the PSD, it will give near zero results in the region where there is only AWGN. Moreover, we also rectify the derivative to make it nonnegative and to move the minimum values beyond the reach of the sEMG signal's bandwidth.

The rectified discrete derivative series of the $\boldsymbol{P}_t$, i.e., $\boldsymbol{D}_t$, is estimated in order to track the amount of changes for each discrete frequency index. To acquire the $\boldsymbol{D}_t$ series, the $\boldsymbol{P}_t$ is subtracted from its one index shifted version and its magnitude is taken as the following:

$$\boldsymbol{D}_t[k] = \left\| \boldsymbol{P}_t[k] - \boldsymbol{P}_t[k-1] \right\|, \tag{27}$$

where $\boldsymbol{P}_t[k-1]$ is the one index shifted version of $\boldsymbol{P}_t$. Thus, $\boldsymbol{D}_t$ gives the slope between each $\boldsymbol{P}_t$ bin. After acquiring the instant slope for the discrete frequency bins, we determine the frequency index where the slope starts to get constant. That is to say, the change in PSD begins to converge to approximately zero.

To smooth out the $\boldsymbol{D}_t$, we utilize a median filter, where the filtered derivative series $\widehat{\boldsymbol{D}_t}$ is given by

$$\widehat{\boldsymbol{D}_t}[k] = median(\boldsymbol{D}_t[k-w], \ldots, \boldsymbol{D}_t[k-w]), \tag{28}$$

where $2w+1$ is the window length of the median filter and the signal $\widehat{\boldsymbol{D}_t}$ is zero-padded accordingly.

Next, we find the index of the minimum of the absolute discrete derivative series $\widehat{\boldsymbol{D}_t}$ with the following equation

$$k_D = \frac{\sum_{k=0}^{K} k \exp(-\widehat{\boldsymbol{D}_t}[k])}{\sum_{k=0}^{K} \exp(-\widehat{\boldsymbol{D}_t}[k])}, \tag{29}$$

which gives greater weights to the smaller values of $\widehat{\boldsymbol{D}_t}$. This value k_D not only approximates the end of the bandwidth of the sEMG signal but is also able to track the muscular fatigue.

1) Effect of the AWGN Power: The power spectra is given by the signal power and the noise power added together. Since the AWGN noise power is equally distributed among the frequency bins in expectation, we get rid of the AWGN content in the rectified discrete derivative series. Hence, let again the signal power be p_s and noise power be p_v. The resulting k_D parameter will be the same whatever the noise power p_v is, or whatever the SNR is. Hence, in both regions when the SNR is high, i.e., $p_v << p_s$, $\frac{p_v}{p_s+p_v} \to 0$, and the SNR is low, i.e., $p_v >> p_s$, $\frac{p_v}{p_s+p_v} \to 1$, we will approximately get the same result from the DDA algorithm, which models the end of the sEMG signal bandwidth.

B. Cumulative Sigmoid Analysis

This method builts upon the first method, where we first calculate the backwards cumulative sum of $\widehat{\boldsymbol{D}_t}$, i.e., $\boldsymbol{C}_t$ for the t^{th} window is calculated as the following:

$$\boldsymbol{C}_t = (\underbrace{\widehat{\boldsymbol{D}_t}[K]}_{1^{st} \text{ index}}, \underbrace{\widehat{\boldsymbol{D}_t}[K] + \widehat{\boldsymbol{D}_t}[K-1]}_{2^{nd} \text{ index}}, \ldots). \tag{30}$$

Hence,

$$\boldsymbol{C}_t[k] = \sum_{k'=0}^{k} \widehat{\boldsymbol{D}_t}[K-k'], \tag{31}$$

for $k \in \{0, 1, 2, \ldots, K\}$.

To determine the index value, where the spectral power starts to converge to a constant, we apply a sigmoid function to $\boldsymbol{C}_t$, which is

$$\boldsymbol{sC}_t[k] = \frac{1}{1 + e^{-\theta(\boldsymbol{C}_t[k] - \Phi(\boldsymbol{C}_t))}}, \tag{32}$$

where $\Phi(.)$ is the geometric mean function. Hence,

$$\Phi(\boldsymbol{C}_t) = \left(\prod_{k=0}^{K} (\boldsymbol{C}_t[k]) \right)^{1/(K+1)}. \tag{33}$$

After the taking the sigmoid of the cumulative sum, the resulting vector would be formed by ones and zeros when

Subject No	Age	Gender	Height (cm)	Weight (kg)
S1	20	Female	167	61
S2	24	Female	169	67
S3	26	Female	165	58
S4	24	Male	173	72
S5	25	Male	178	68
S6	28	Male	168	70
S7	24	Male	167	72
S8	25	Male	189	66
S9	24	Male	175	78
S10	24	Female	181	60

Table I: Gender, age, height, weight information of the subjects

Figure 1: Visual of the sEMG Data Acquisition System.

θ is allowed to go to infinity, i.e., $\theta \to \infty$. Let the index of transition from zero to one be k^+. This index gives the index, where the spectral power starts to decrease and converge to a constant, which is given by

$$k_C = K - k^+. \tag{34}$$

1) Effect of the AWGN Power: Let again the signal power be p_s and noise power be p_v. Since CSA utilizes DDA, the resulting k_C parameter will be the same whatever the noise power p_v is, or whatever the SNR is, for the same reasons as the previous section. Hence, in both regions when the SNR is high, i.e., $p_v << p_s$, $\frac{p_v}{p_s+p_v} \to 0$, and the SNR is low, i.e., $p_v >> p_s$, $\frac{p_v}{p_s+p_v} \to 1$, we will get approximately the same result from the CSA algorithm, which again models the end of the sEMG signal bandwidth.

V. Experiments

In this section, we compare the proposed spectrum based fatigue tracking metrics in Sections IV-A and IV-B, i.e., Discrete Derivative Analysis (DDA) and Cumulative Sigmoid Analysis (CSA), with the state of the art metrics in Sections III-A, III-B, III-C and III-D, i.e., Mean Frequency, Band-limited Mean Frequency, Median Frequency and Band-limited Median Frequency. For this purpose, an appropriate setup needs to be provided in order to sufficiently collect correct EMG signals under muscular fatigue circumstances. In the following subsection, Section V-A, the experiment setup is detailed along with the wearable sEMG data acquisition system, type of physical activities, and information about the subjects. In the rest of this section, we experiment on the two important considerations we need to make for our fatigue metrics, which were detailed in Section II-C.

For the first consideration, in Section V-B, the proposed methods are compared to the state of the art to validate that our methods are indeed appropriate for use in fatigue tracking and they closely represent and model the muscular fatigue at least in the behavioral sense.

Next, for the second consideration, in Section V-C, the effect of increasing AWGN power on all of the fatigue tracking methods are shown to study whether or not the estimated metrics from the noisy signals can closely represent the true metrics.

A. Experimental Setup

For the experiments in order to validate and compare all the mentioned methods, EMG data needs to be collected during activities that substantially increases the fatigue level in muscles. Such activities mostly require a physical motion, in which the sensor electrodes might lose the contact with the skin or wirings can limit the movement. To overcome such obstacles, we embedded an 8 channel wireless EMG data acquisition system into a compressive sports garment, which is seen in Figure 1.

The surface EMG sensors follow the basic dry active sEMG architecture. The copper core, gold plated, disk shape electrodes are manufactured and localized according to the SENIAM standards, which is 10mm diameter and 20mm inner electrode distance [30]. The difference of the voltage levels in the electrodes are taken via an instrumentation amplifier followed by a quasi highpass filter and gain amplifier to obtain a complete gain of 500. Finally the output of the gain is put through a band-pass filter with cutoff frequencies of 20-450Hz.

The sensor outputs are sent to a core unit via textile based litz wire cables, which enable high flexibility and stretchability. In the core unit, 8 different sensor outputs are sampled simultaneously with a 12-bit ADC resolution and 1kHz sampling rate. Then, the gathered data is transmitted to MatLab interface via WiFi.

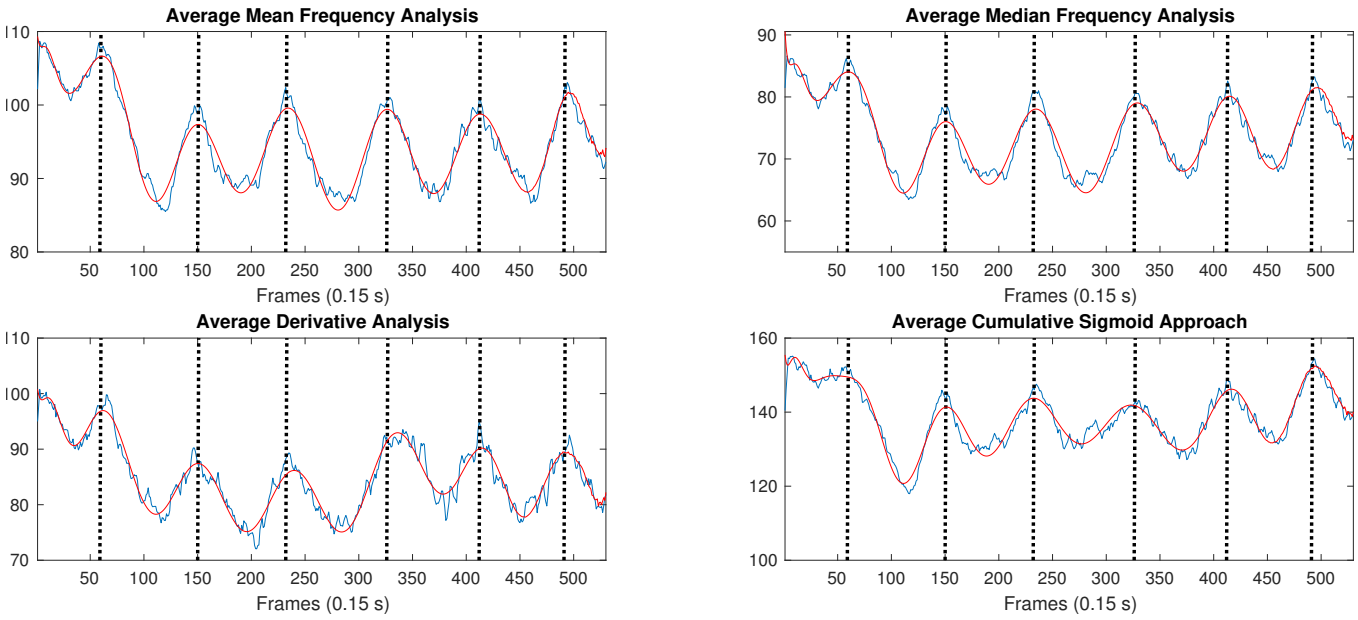

Figure 2: Average mean frequency, median frequency, discrete derivative metric, cumulative sigmoid metrics in the experiments.

The sEMG sensors are covered with epoxy in order to provide sealing and robustness. sEMG sensors are placed on specific quadriceps muscles, which are Vastus Medialis, Rectus Femoris and Vastus Lateralis with correct directions and locations [30]. Also, the vibration-preventing compressiveness in the tight provides a suitable platform for measuring the activities that create motion artifacts.

In our experiments, sEMG data is gathered from 10 healthy subjects with various physical properties (i.e. age, gender, height (cm) and weight (kg)), detailed in Table I. During the experiments, subjects realized dumbbell squats of 7 sets with 2.5 kilograms in each hand, where they stand up straight while holding a dumbbell on each hand (palms facing the side of their legs).

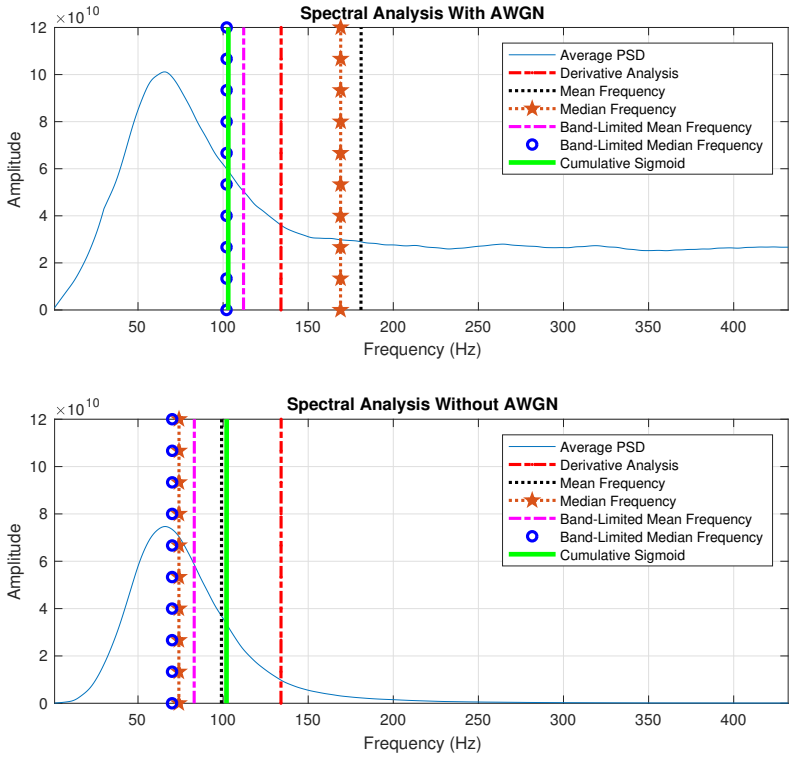

Figure 3: The plots of the results of the methods on average PSD with low SNR (top) and high SNR (bottom).

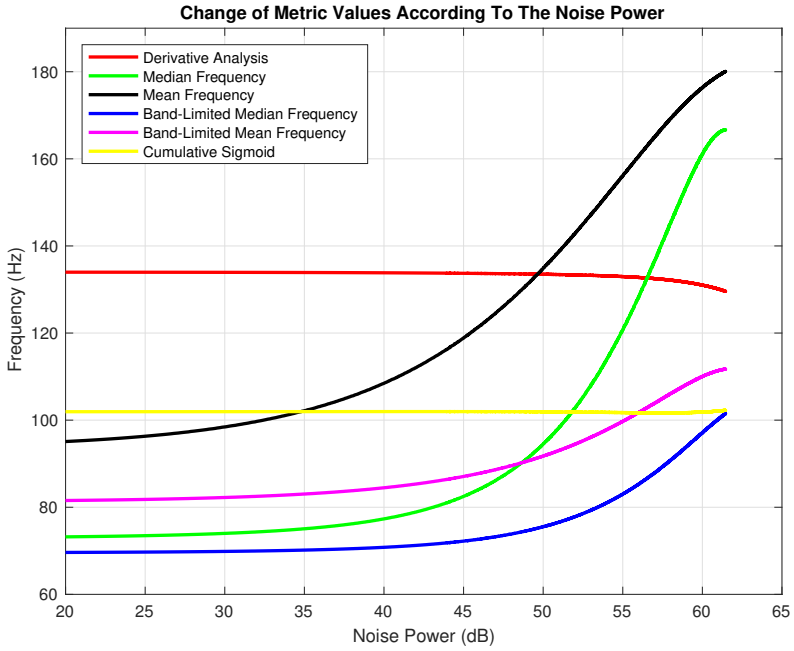

Figure 4: The effect of AWGN power on all of the methods.

B. Validation of Proposed Fatigue Models

In this first part of the experiments, we validate our presented methods DDA (in Section IV-A) and CSA (in Section IV-B). For validation, we compared our methods to the methods in Sections III-A, III-C. First, we have collected the EMG from each of our subjects through our data acquisition system. Then, the collected EMG data has been fed to the contraction detection algorithm in Section II-B. The parts of the signal that were detected as contractions include the sEMG signals. Hence, these parts of the signal (i.e., frames) are used in the calculation of our metrics DDA, CSA and the metrics Mean Frequency and Median Frequency. This has been done for all of the subjects. After that, the metrics gathered from all of the subjects are normalized, synchronized and finally averaged.

In Figure 2, the average results and smoothed results are displayed. As can be seen, each metric used in or experiments conforms to a similar behavior throughout the contraction frames. They all have the same pattern, which means that our introduced methods are suitable to track muscular fatigue since mean and median frequencies are well established metrics in fatigue tracking. DDA especially shows a remarkable similarity to the mean and median frequency. In that regard, DDA approach may be able to better model the fatigue than CSA.

C. Effect of AWGN Power on The Spectral Shift Methods

For the second part of the experiments, in this subsection, AWGN noise is gradually added to simulate its effect on the fatigue tracking methods.

We artificially add AWGN noise to the EMG data to simulate the effect of the AWGN noise power on the fatigue tracking methods. Their results are shown in Figures 3 and 4.

In Figure 3, we see that after the addition of the AWGN noise, the changes were the following:

- Mean Frequency: ≈ 100 Hz $\rightarrow \approx 180$ Hz,
- BL Mean Frequency: ≈ 85 Hz $\rightarrow \approx 110$ Hz,
- Median Frequency: ≈ 75 Hz $\rightarrow \approx 170$ Hz,
- BL Median Frequency: ≈ 70 Hz $\rightarrow \approx 100$ Hz,
- Discrete Derivative: ≈ 135 Hz $\rightarrow \approx 135$ Hz,
- Cumulative Sigmoid: ≈ 100 Hz $\rightarrow \approx 100$ Hz,

where BL is used for 'Band-Limited'. As can be seen, while Mean Frequency, Band-Limited Mean Frequency, Median Frequency and Band-Limited Median Frequency have drastically changed under increased AWGN (i.e., low SNR), our metrics Discrete Derivative and Cumulative Sigmoid have more or less remained the same. Henceforth, they are successful in retaining their modeling capabilities under increased noise. Moreover, because the effect of the AWGN has been little to none for our metrics, we can say that our methods are very robust against AWGN.

Furthermore, in Figure 4, we illustrate the outputs of our methods and the state-of-the-art together under gradual increase of noise power. As expected, aside from our two approaches, outputs of the state-of-the-art changes with the AWGN noise level present in the signal, consequently hindering our ability to correctly interpret the outputs as fatigue levels. Mean frequency metric (whether band-limited or not) is affected gradually starting from a relatively small noise power. It seems the band limited version of the metric can resist the effects of the increased noise power better. Nevertheless, the noise power increase substantially affects the metric value. The median frequency seems to be able to better deal with the noise power compared to the mean frequency, at least in the lower noise power regions. However, the effect of the noise power starts to show itself after a sufficient level and its distortion quickly catches up with the distortion in the mean frequency. Henceforth, median frequency as well has

insufficient robustness against the increased AWGN power.

On the other hand, our metrics deal with the increase in the noise power substantially better than the conventional metrics. The distortion in the Discrete Derivative metric remains less than a few Hz even under very low SNR scenarios. Cumulative Sigmoid metric shows an even better resistance. Remarkably, it seems the increased noise power has little to no effect, however large it is. Thus, we can clearly see that our metrics are much more robust than the conventional metrics for tracking fatigue under high or changing noise power situations.

VI. Conclusion

In this paper, we have introduced novel metrics that can accurately capture the spectral shift in sEMG signals to track muscle fatigue. With their increased modeling capabilities, our metrics can more accurately capture the muscular fatigue. Compared to the conventional techniques for modeling the fatigue and tracking the spectral shift of the signal, our methods are very robust to the AWGN noise power in the environment. While the conventional techniques are highly affected by the AWGN power present in the signal, in comparison, its effects on our metrics are negligible.

References

[1] H. Liu, "Exploring human hand capabilities into embedded multifingered object manipulation," *IEEE Transactions on Industrial Informatics*, vol. 7, no. 3, pp. 389–398, Aug 2011.

[2] R. Chattopadhyay, M. Jesunathadas, B. Poston, M. Santello, J. Ye, and S. Panchanathan, "A subject-independent method for automatically grading electromyographic features during a fatiguing contraction," *IEEE Transactions on Biomedical Engineering*, vol. 59, no. 6, pp. 1749–1757, June 2012.

[3] Y. Fan and Y. Yin, "Active and progressive exoskeleton rehabilitation using multisource information fusion from emg and force-position epp," *IEEE Transactions on Biomedical Engineering*, vol. 60, no. 12, pp. 3314–3321, Dec 2013.

[4] R. I. Pettigrew, W. J. Heetderks, C. A. Kelley, G. C. Y. Peng, S. H. Krosnick, L. B. Jakeman, K. D. Egan, and M. Marge, "Epidural spinal stimulation to improve bladder, bowel, and sexual function in individuals with spinal cord injuries: A framework for clinical research," *IEEE Transactions on Biomedical Engineering*, vol. 64, no. 2, pp. 253–262, Feb 2017.

[5] B. J. E. Misgeld, M. Lüken, R. Riener, and S. Leonhardt, "Observer-based human knee stiffness estimation," *IEEE Transactions on Biomedical Engineering*, vol. 64, no. 5, pp. 1033–1044, May 2017.

[6] X. Navarro-Sune, A. L. Hudson, F. D. V. Fallani, J. Martinerie, A. Witon, P. Pouget, M. Raux, T. Similowski, and M. Chavez, "Riemannian geometry applied to detection of respiratory states from eeg signals: The basis for a brain;ventilator interface," *IEEE Transactions on Biomedical Engineering*, vol. 64, no. 5, pp. 1138–1148, May 2017.

[7] K. M. Vamsikrishna, D. P. Dogra, and M. S. Desarkar, "Computer-vision-assisted palm rehabilitation with supervised learning," *IEEE Transactions on Biomedical Engineering*, vol. 63, no. 5, pp. 991–1001, May 2016.

[8] M. Sartori, D. G. Llyod, and D. Farina, "Neural data-driven musculoskeletal modeling for personalized neurorehabilitation technologies," *IEEE Transactions on Biomedical Engineering*, vol. 63, no. 5, pp. 879–893, May 2016.

[9] Y. Bai, D. Do, Q. Ding, J. A. Palacios, Y. Shahriari, M. M. Pelter, N. Boyle, R. Fidler, and X. Hu, "Is the sequence of superalarm triggers more predictive than sequence of the currently utilized patient monitor alarms?" *IEEE Transactions on Biomedical Engineering*, vol. 64, no. 5, pp. 1023–1032, May 2017.

[10] E. Gaeta, G. Cea, M. T. Arredondo, and J. P. Leuteritz, "Amirtem: A functional model for training of aerobic endurance for health improvement," *IEEE Transactions on Biomedical Engineering*, vol. 59, no. 11, pp. 3155–3161, Nov 2012.

[11] M. Ergeneci, K. Gokcesu, E. Ertan, and P. Kosmas, "An embedded, eight channel, noise canceling, wireless, wearable semg data acquisition system with adaptive muscle contraction detection," *IEEE Transactions on Biomedical Circuits and Systems*, vol. 12, no. 1, pp. 68–79, Feb 2018.

[12] G. Robertson, G. Caldwell, J. Hamill, G. Kamen, and S. Whittlesey, *Research methods in biomechanics, 2E*. Human Kinetics, 2013.

[13] A. V. Boxtel and L. R. B. Schomaker, "Motor unit firing rate during static contraction indicated by the surface emg power spectrum," *IEEE Transactions on Biomedical Engineering*, vol. BME-30, no. 9, pp. 601–609, Sept 1983.

[14] M. M. Lowery and M. J. O'Malley, "Analysis and simulation of changes in emg amplitude during high-level fatiguing contractions," *IEEE Transactions on Biomedical Engineering*, vol. 50, no. 9, pp. 1052–1062, Sept 2003.

[15] R. Merletti and D. Farina, *Muscle Force and Myoelectric Manifestations of Muscle Fatigue in Voluntary and Electrically Elicited Contractions*. Wiley-IEEE Press, 2016, pp. 592–. [Online]. Available: http://ieeexplore.ieee.org/xpl/articleDetails.jsp?arnumber=7471089

[16] E. Koutsos and P. Georgiou, "An analogue instantaneous median frequency tracker for emg fatigue monitoring," in *2014 IEEE International Symposium on Circuits and Systems (ISCAS)*, June 2014, pp. 1388–1391.

[17] B. H. Zhou, P. Liu, N. B. Liu, X. H. Wu, R. Lu, and X. M. Ni, "Median frequency of surface emg signal of antagonist muscles during repeated contractions," in *1992 14th Annual International Conference of the IEEE Engineering in Medicine and Biology Society*, vol. 4, Oct 1992, pp. 1626–1627.

[18] A. J. Fuglevand, D. A. Winter, A. E. Patla, and D. Stashuk, "Effect of increased motor unit action potential duration on the amplitude and mean power frequency of the electromyogram," in *Images of the Twenty-First Century. Proceedings of the Annual International Engineering in Medicine and Biology Society,*, Nov 1989, pp. 953–954 vol.3.

[19] S. R. Alty and A. Georgakis, "Mean frequency estimation of surface emg signals using filterbank methods," in *2011 19th European Signal Processing Conference*, Aug 2011, pp. 1387–1390.

[20] R. Merletti, D. Biey, M. Biey, G. Prato, and A. Orusa, "On-line monitoring of the median frequency of the surface emg power spectrum," *IEEE Transactions on Biomedical Engineering*, vol. BME-32, no. 1, pp. 1–7, Jan 1985.

[21] K. Gokcesu, M. Ergeneci, E. Ertan, A. Z. Alkilani, and P. Kosmas, "An semg-based method to adaptively reject the effect of contraction on spectral analysis for fatigue tracking," in *Proceedings of the 2018 ACM International Symposium on Wearable Computers, UbiComp 2018, Singapore, Singapore, October 8-12, 2018*, 2018, pp. 80–87. [Online]. Available: http://doi.acm.org/10.1145/3267242.3267292

[22] O. Sayli and A. Akin, "Investigation of the usage of averaged instantaneous frequency parameter along with mean and median frequency in electromyogram (emg) analysis," in *Proceedings of the IEEE 13th Signal Processing and Communications Applications Conference, 2005.*, May 2005, pp. 597–600.

[23] R. B. R. Manero, A. Shafti, B. Michael, J. Grewal, J. L. R. Fernández, K. Althoefer, and M. J. Howard, "Wearable embroidered muscle activity sensing device for the human upper leg," in *2016 38th Annual International Conference of the IEEE Engineering in Medicine and Biology Society (EMBC)*, Aug 2016, pp. 6062–6065.

[24] S. S. Nair, R. M. French, D. Laroche, and E. Thomas, "The application of machine learning algorithms to the analysis of electromyographic patterns from arthritic patients," *IEEE Transactions on Neural Systems and Rehabilitation Engineering*, vol. 18, no. 2, pp. 174–184, 2010.

[25] M. Khezri and M. Jahed, "Real-time intelligent pattern recognition algorithm for surface emg signals," *Biomedical engineering online*, vol. 6, no. 1, p. 1, 2007.

[26] X. Zhang, X. Chen, Y. Li, V. Lantz, K. Wang, and J. Yang, "A framework for hand gesture recognition based on accelerometer and emg sensors," *IEEE Transactions on Systems, Man, and Cybernetics-Part A: Systems and Humans*, vol. 41, no. 6, pp. 1064–1076, 2011.

[27] S. Karlsson, J. Yu, and M. Akay, "Time-frequency analysis of myoelectric signals during dynamic contractions: a comparative study," *IEEE transactions on Biomedical Engineering*, vol. 47, no. 2, pp. 228–238, 2000.

[28] M. Cifrek, S. Tonković, and V. Medved, "Measurement and analysis of surface myoelectric signals during fatigued cyclic dynamic contractions," *Measurement*, vol. 27, no. 2, pp. 85–92, 2000.

[29] K. Gokcesu, M. Ergeneci, E. Ertan, and H. Gokcesu, "An adaptive algorithm for online interference cancellation in emg sensors," *IEEE Sensors Journal*, pp. 1–1, 2018.

[30] SENIAM, "Sensor placement," http://www.seniam.org/bicepsbrachii.html.